Journal of Physics D: Applied Physics

Whispering gallery mode microlaser based on single polymer fiber fabricated by electrospinning

To cite this article before publication: Xianxian Chen *et al* 2019 *J. Phys. D: Appl. Phys.* in press https://doi.org/10.1088/1361-6463/ab39f1

IOP Publishing Journal Title
Journal **XX** (XXXX) XXXXXX https://doi.org/XXXX/XXXX

Whispering gallery mode microlaser based on single polymer fiber fabricated by electrospinning

Xianxian Chen[1,†], Kang Xie[1,†], Taoping Hu[2,†], Xiaojuan Zhang[4,†], Yong Yang[4], Jiajun Ma[3], Junxi Zhang[1], Xusheng Cheng[5] and Zhijia Hu[1,3,4,*]

1School of Instrument Science and Opto-electronics Engineering, Hefei University of Technology, Hefei, Anhui 230009, P. R. China
2College of Science, Nanjing Forestry University, Nanjing, Jiangsu 210037, P. R. China
3State Key Laboratory of Environment-Friendly Energy Materials, Southwest University of Science and Technology, Mianyang, Sichuan 621000, P.R. China
4Aston Institute of Photonic Technologies, Aston University, Birmingham B4 7ET, United Kingdom
5Department of Computer and Information, Hefei University of Technology, Hefei, Anhui 230009, P.R. China

[†]*Xianxian Chen, Kang Xie, Taoping Hu and Xiaojuan Zhang contributed equally to this work*

E-mail: E-mail: zhijiahu@hfut.edu.cn
Received xxxxxx
Accepted for publication xxxxxx
Published xxxxxx

Abstract

Electrospinning is a very simple method of preparing polymer solutions into high performance fibers. In this work, PM597-doped polymer fibers with different diameters have been fabricated by electrospinning technology. Whispering gallery mode (WGM) lasing emission has been observed when a 532 nm pulse laser beam radially excited the single electrospun polymer fiber (EPF). The distribution of WGMs is also quantitatively confirmed through theoretical calculation. In addition, the number of WGM laser peaks decreases as the diameter of the EPF decreases. Single longitudinal mode laser emission can be obtained when the EPF diameter decreases to 8.8 μm. It has also been found that WGM laser from single EPF have relatively low thresholds and good lifetime compared to droplets or other fiber lasers. Moreover, EPF networks have unique research prospects in photonic devices, optical pump lasers, and biosensing due to their very large surface to volume ratio.

Keywords: laser, whispering gallery mode, polymer fiber, electrospinning

1. Introduction

The resonant microcavity as a basic element of lasing generation can be summarized as whispering gallery mode (WGM), photonic crystal defect, Fabry-Perot (F-P), and distributed feedback (DFB) resonant microcavities [1,2]. Among all of these resonators, WGM confines the light near a circular ring boundary by total internal reflection. In addition, WGM reasonable microcavity has been extensively studied due to the advantages of inherently high quality (Q) factor, low mode volume, enhanced optical field, relatively simple fabrication, very narrow spectral linewidth, and a large optical density [3-8]. In 1961, WGM microspherical laser resonator was firstly observed by C. G. Garrett in the spherical sample of CaF_2: Sm^{++} [9]. In recent years, WGM lasing from dye-doped microstructure system has been realized. Hee-Jong Moon *et al.* have investigated the lasing property of the WGMs existing in a square microcavity with round corners [10]. V. V. Ursaki *et al*. have reported the high Q WGM lasing resonators in hexagonal ZnO microdiscs produced by metal–organic chemical vapour deposition [11]. So far, a variety of structures have been proven to sustain WGMs, such as microspheres, hemispheres, microdisks, microtubules, optical fibers, microbubbles, micropillars, and microtoroids [1,2]. Meanwhile, with the development of science and technology, various methods for manufacturing WGM resonators have emerged. Traditionally, solid-state semiconductor microcavities are manufactured based on top-down or bottom-up technologies with sophisticated manufacturing techniques, but they rely heavily on complex control parameters [12]. Flexible soft matter microcavities are formed by surface tension-induced self-assembly methods [13-15]. Van. D. Ta *et al*. have fabricated polymer

droplets with WGM laser emission by using this method, and clearly demonstrated the tuning laser mode by mechanical deformation [13]. Although the method of self-assembled microcavity proposed by Van. D. Ta *et al*. is simple and low-cost, it cannot be mass-produced. Alternatively, the microcavity can be fabricated by sol-gel wet chemical synthesis techniques [16]. Y. Yang *et al*. have used sol-gel coating technology to introduce Er^{3+} ions into the wall of a microbubble resonator and achieved lasing light in the 1550 nm band [17]. Recently, electrospinning technology has attracted extensive interests of researchers due to its high-throughput fabrication on the polymer fiber (PF) networks, low-cost, and various ways to control the properties of fiber materials [18-20]. D. Huang *et al.* have fabricated polyvinyl alcohol nanofibers doped with Rhodamine 6G laser dyes by electrospinning technique and found that the intensity of the random lasers increases with increasing dye concentration [21]. S. Krämmer`s group has reported that electrospun R6G doped PMMA fibers feature deterministic laser emission and has identified ring resonators to be responsible for comb-like laser spectra [18]. However, so far, most reports about WGM lasers have some shortcomings like high threshold and low lifetime, which hinders the application of WGM resonators in the field of sensors and optoelectronic devices [2,13,18,22,23].

In this work, we fabricate some electrospun polymer microcavities with the diameters ranging from 5 to 30 μm. The microcavities are uniformly formed during the manufacturing process and the fiber network geometry is different from other artificially designed polymer cavities. When pumping a single EPF, the mechanism of lasers is carefully studied and found to be attributed to WGM lasers. In particular, it has been observed that the threshold of WGM lasers is lower than Refs. [1], [12], [14]. Besides, single longitudinal mode emission can be obtained from dyes-doped EPF with diameter of ~8.8 μm. When the lasing emission collected device (location aperture) is some extent away from the pump source, non-lasing can be detected, which further proves the lasing is from WGM cavity. In addition, the electrospinning technology fabricating WGM laser provides a new platform for sensors and integrated photonic devices.

2. Materials and methods

The randomly distributed EPFs used in our experiment were fabricated by using advanced electrospinning technology. Electrospinning sample solution is a mixture of poly(methyl methacrylate) (PMMA), Pyrromethene 597 (PM597) in acetone. The concentration of PM597 and PMMA are around 0.4 wt % and 38 wt %, respectively. Preparation of electrostatic spinning process [24,25]: A high voltage power supply is used to provide high voltages in the range of -30-50 kV. The spinning solution is carefully loaded in a 5 mL syringe, and a stainless steel capillary metal needle hub with a 0.9 mm inner diameter is attached to the syringe. The positive pole of the high voltage power supply is connected to the tip of the needle. The grounded electrode is connected to a metal collector covered with foil sheet (5×10 cm). A fixed electrical potential of 12 kV is applied across a distance of 20 cm between the needle tip and the collector. The feed rate of solutions is controlled at 0.08 mm/min through a single syringe pump. Figure 1 shows the microscope images of PM597-doped PMMA fiber network via electrospinning. As shown in Fig. 1(a), the random distribution of EPFs are clearly visible. Under higher magnification in Fig. 1(b), it shows clearly the location of the 532 nm ns laser pumped area for single EPF. It should be noted that the parallel aligned fringes come from foil substrate. Figure. 1(c) shows a scanning electron microscopy (SEM) graph corresponding to the EPF sample. The randomly oriented fibers have a diameter of 5-25 μm, the majority of the fiber diameter is distributed between 6-16 um (Fig. 1(e)). A partial SEM images of a single EPF is shown in Fig. 1(d).

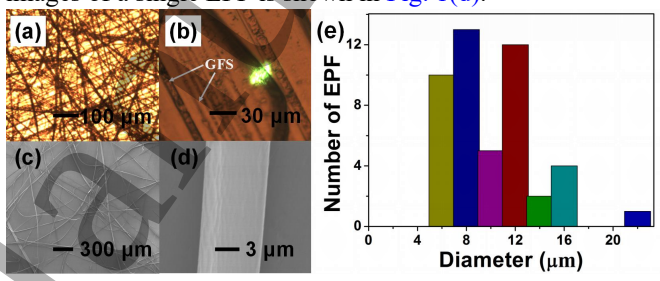

Figure 1. (a) the images of disorderly arranged EPF networks, (b) 532 nm ns laser pumped single EPF. The parallel aligned fringes are the grains of foil sheet (GFS), (c) SEM images of randomly oriented EPF, (d) SEM picture of a single EPF, (e) diameter distribution of the EPFs corresponding to the SEM images of (c).

Figure 2 shows the microscope measurement setup based on the micro spectrum system coupling with pumping laser. A Q-switched Nd:YAG laser which outputs wavelength of 532 nm with a round spots (pulse duration 10 ns, repetition rate 10 Hz, spot diameter 30 μm) is used as pumping source. The pump pulse energy and polarization are controlled by a Glan Prism group. Two mirrors are used to change the pumping laser path to dichroic mirror of the micro spectrum system. The pumping laser is focused onto the sample passes through a 532 nm total reflection dichroic mirror and a focused objective. The signal emitted from EPF is collected with microscope objective and guided to a beam splitter where 50% of the lasing emission is sent to the CCD camera to obtain an image of the sample. The remaining 50% of the laser emission passes through the polarizer and is received by a common fiber, the polarization of the WGM lasing emission is checked by rotating the polarizer. The angle between the polarization direction of the polarizer and the Y-axis is defined as θ, and the initial angle is zero [18,26]. We use a 1*2 multimode fiber coupler to connect fiber spectrometer (QE65PRO, Ocean Optics, resolution ~0.4 nm,

integration time 100 ms), halogen lamp and common fiber. The Port 1(2) is connected to spectrometer (halogen lamp). The common fiber is multi fiber structure including outer fiber and inner fiber section. The yellow dot ring in the outer section light is from Port 2 to make sure the collection location. We move the yellow dot ring to change the internal collection aperture position to collect laser emissions in the different location along the EPF.

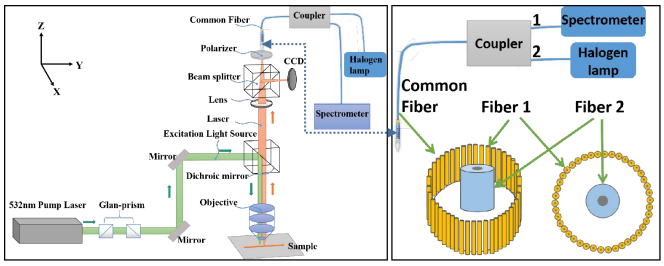

Figure 2. The microscope measurement setup for the EPF.

3. Results and discussions

Figure 3 describes WGM characteristic measurement of a typical single EPF with diameter of ~20.7 μm. As shown in Fig. 3(a), the lasing intensity increases with increasing pump energy. For the pump energy below 0.4 μJ, weak and extensive spontaneous emission from the EPF can be observed. When the pump energy reaches 0.4 μJ, the initial sharp peaks occur from the broad emission and their intensity increases significantly with the pump energy. The non-linear variations between input and output energy of the lasing peak is shown in Fig. 3(b). The apparent transition from spontaneous emission to stimulated emission and the non-linear increase in emission intensity demonstrate the lasing emission action, and the threshold of the lasing is approximately 0.4 μJ. The main lasing peak locates at 574.26 nm with the FWHM of ~0.3 nm. In addition, we studied the laser thresholds for fibers of different diameters and found that the threshold does not vary linearly with diameter.

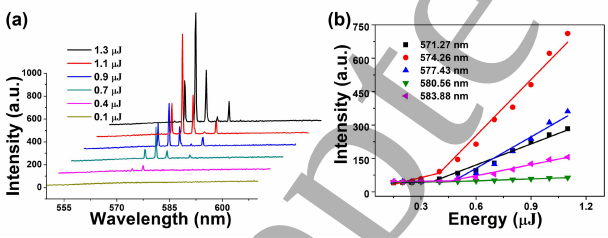

Figure 3. (a) Emission spectra of single EPF with different pumping energy. (b) Emission intensity as a function of pumping energy.

The polarization characteristics of the WGM lasing emission depend on the direction of propagation of the pump beams in the fiber, and there are two polarization modes (transverse magnetic (TM) or transverse electric (TE)). When the electric field is parallel (perpendicular) to the length axis of the fiber, the lasing emission is a transverse magnetic TM (TE) wave that forms a special axially (radially) polarizzation emission [27,28]. In order to study the polarization state of the WGM laser from the EPF, we analyzed the polarization of the lasing emission by using the polarization measuring device of Fig. 2. The θ with 0 is defined as the polarization direction of the polarizer paralleling Y-axis. Figure 4(a) shows the lasing intensity change with θ by rotating the polarizer. The lasing emission intensity reaches its maximum when polarizer is set along the Y-axis (θ = 0° and 180°). It is clear that this phenomenon is very consistent with Malus's law ($I=Io(cos^2\theta)$), thus demonstrating that the lasing emission is only TM mode. In order to determine the laser mechanism, we further analyzed the laser characteristics. The lasing modes (m) can be calculated from the following formula [4, 29-31]:

$$\lambda^{-1}(R,n_1,n_r,r,m)=\frac{1}{2\pi R n_1}\left[m+\frac{1}{2}+2^{-\frac{1}{3}}a(r)\left(m+\frac{1}{2}\right)^{\frac{1}{3}}\frac{L}{\left(n_r^2-1\right)^{\frac{1}{2}}}+\frac{3}{10}2^{\frac{2}{3}}a^2(r)\left(m+\frac{1}{2}\right)^{-\frac{1}{3}}-2^{-\frac{1}{3}}L\left(n_r^2-\frac{2}{3}L^2\right)\frac{a(r)\left(m+\frac{1}{2}\right)^{-\frac{2}{3}}}{\left(n_r-1\right)^{\frac{3}{2}}}\right] \quad (1)$$

where λ is the resonant wavelength, R is the radius of the EPF microcavity, n_1 is the refractive index of EPF, n_2 is the refractive index surrounding medium, $n_r = n_1/n_2$. L is the polarization characteristic coefficient, $L = n_r$ for TE modes, and $L = n_r^{-1}$ for TM modes. a(r) are the roots of the Airy function, where r is the radial mode number, and m is the mode number. The diameter of a single fiber in our experiment is ~20.7 μm, the refractive index of EPF and surrounding air are 1.487 (n_1) and 1 (n_2), respectively. The theoretical calculation indicates that the WGM peaks belong to the first-order (r=1) TM mode, and the corresponding mode numbers m are found to be 154-158. These values closely match the laser peaks in the corresponding spectra shown in Fig. 4, thus validating the WGM lasing emission mechanism.

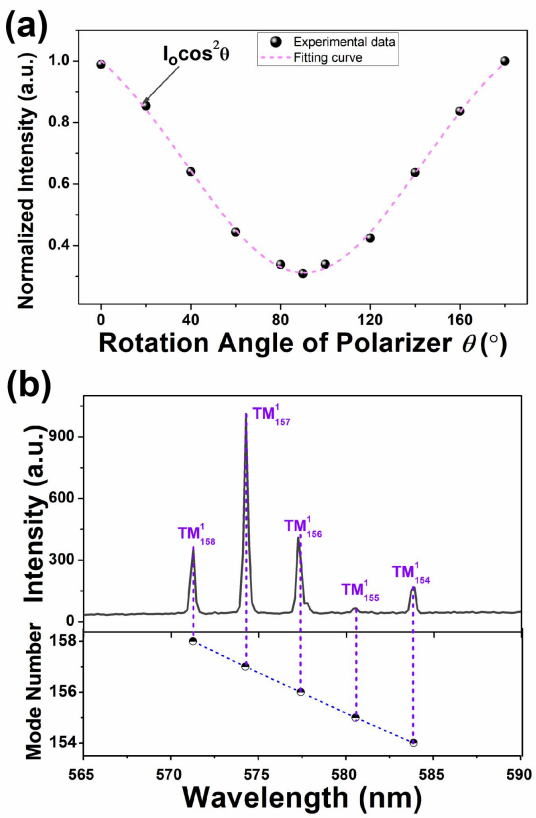

Figure 4. (a) The lasing intensity as a function of rotation angle of polarizer. (b) Spectrum of the EPF under excitation and mode allocation.

In order to obtain more information about the lasing properties, single EPF with different diameters are measured. Figure 5 illustrates series of lasing spectra from single EPF with different diameters. The intensity of the pump laser is fixed at 0.3 μJ. It can be clearly seen from the spectra that the free spectral range (FSR) increases and the number of laser peaks decreases from 8 to 1 as EPF diameter decreases. In addition, the lasing envelope shifts from 589.5 to 567.5 nm as the diameter of the single EPF decrease from 26.1 μm to 8.8 μm. This may be due to the fact that the smaller diameter EPF has a lower effective dye concentration which will result in inhibiting the re-absorption and re-emission (Stokes shift), or a change in factors such as coupling efficiency, two-photon absorption. As a result, the lasing envelope shift towards shorter wavelengths [32,33]. The peak of the single longitudinal mode lasing emission locates in 564 nm with the linewidth of 0.3 nm. Furthermore, the calculated laser mode number is 190 corresponding to diameter of 8.8 μm. We have found that the acquisition of a single longitudinal mode laser is closely related to the cavity size.

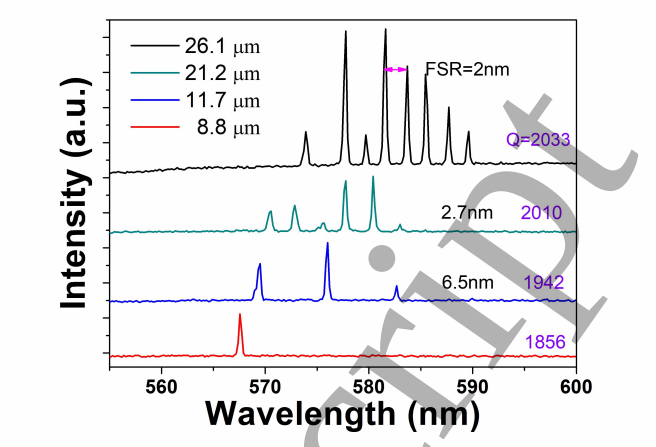

Figure 5. Lasing spectra from single EPF with different diameter.

To further investigate the characteristics of the WGM lasing axial transmission along EPF, we measure the lasing emission emitted at different receiving locations. A schematic diagram of the measurement system is shown in Fig. 2. Figures 6(a)-(f) clearly show the pump and collected position for the single EPF, where the yellow dot ring light is the positioning aperture of outer fiber section, and there is dark collection aperture inner the yellow dot ring right. The green dot is pump location. And yellow dot light ring is from the halogen lamp. The axial direction of the EPF is shown in Fig. 6(a). In Fig. 6(d), the pumped EPF is at the center of the collected aperture, and the intensity of the received lasing is the strongest, as shown by the blue line in Fig. 6(g). However, when the positioning hole is moved along the axial direction of the EPF to the position shown in Fig. 6(e), the spectrum of the lasing is as shown by the green line in Fig. 6(g), and it is apparent that the intensity of the laser is weakened. When the pumped EPF is not in the aperture (Fig. 6(f)), the laser is not detected, as shown by the pink line in Fig. 6(g). The same phenomenon was found when the aperture moved along the EPF to a symmetrical position (Fig. 6(b), (c)), as shown by the red and black curves in Fig. 6(g). This indicates that lasing occurs only in the pumped WGM microcavity region. In other words, the WGM lasing cannot be transmitted in the axial direction of the fiber, which further proves the WGM mechanism. In addition, the slight shift of the laser peaks in Fig. 6(c), (d), and (e) may be due to a small change in the diameter of the EPF [34].

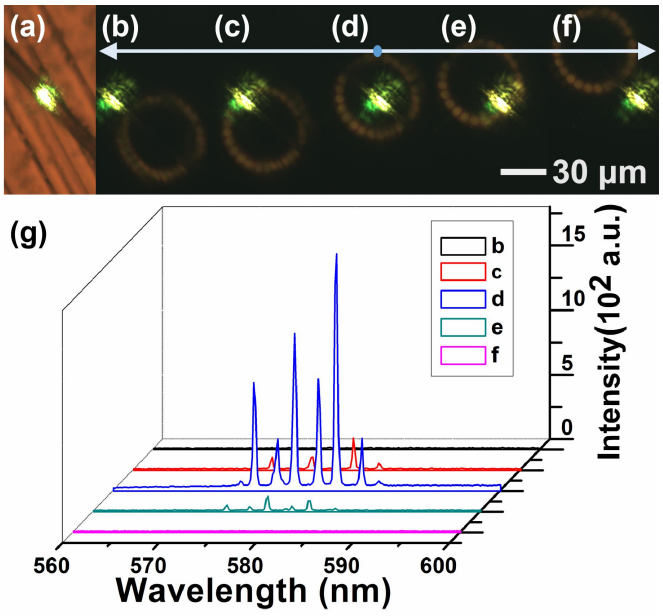

Figure 6. (a)-(f) Optical image of the measured single EPF, (g) spectrogram corresponding to (b)-(f), the black, red, blue, green, and pink curves represent the detected laser spectra of b, c, d, e, and f, respectively.

Figure 7 depicts the WGM lasing lifetime for PM597-doped EPF at pump energy of 0.35 μJ. The WGM Laser intensity decreased to 83.5% after 80 minutes pulses pump. Obviously, the laser intensity decreased faster after 80 minutes pulses pump, but the laser intensity was still as high as 77.41% after 120 minutes pulses pump. However, so far, WGM lasing with long life has not been reported in various resonant microcavities, such as spherical or cylindrical [3,12,35]. In general, a polymer WGM resonant microcavity with good lifetime was produced for the first time by electrospinning technology.

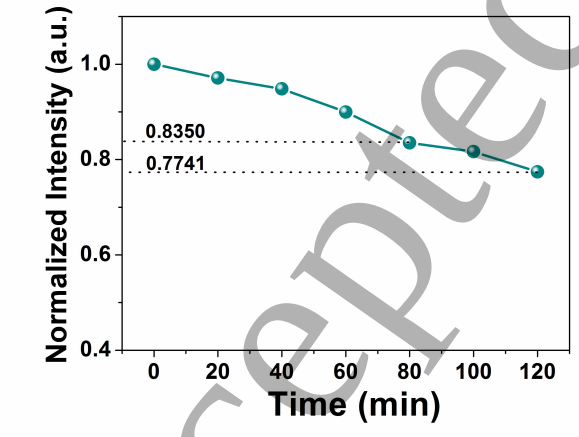

Figure 7. The normalized integrated intensity of the peaks versus pump times for EPF.

Conclusion

In conclusion, we fabricate PM597-doped polymer fibers with different diameters using electrospinning technology. Multimode and even single longitudinal mode laser is observed from EPF under laser pumping. Whispering gallery mode lasing emission has been proved by analysing the lasing spectrum from the single EPF. In addition, the polarization characteristics of the WGM lasing are systematically investigated using microscope measuring device, which is in good agreement with the theoretical calculation. Furthermore, the number of WGM lasing peaks decreases as the diameter of the EPF decreases. It is also found that EPFs has relatively low thresholds compared to droplets or other fibers. We have demonstrated that the WGM lasing excited by the radial vertical pump EPF cannot be transmitted in the axial direction by moving the lasing receiving device (positioning aperture). In our work, electrospinning technology is a simple, versatile and particularly low-cost technology that requires only a small volume of material to fabricate WGM lasing with a complex spatial structure. EPFs have unique application prospects in the field of photonic devices and biological sensing.

Acknowledgements

The authors would like to thank the financial supports from National Natural Science Foundation of China (11874012, 11404087, 11574070, 51771186, 11404086, 11874126, 61501165); Fundamental Research Funds for the Central Universities ((JZ2019HGPA0099; PA2018GDQT0006); Project of State Key Laboratory of Environment-friendly Energy Materials, Southwest University of Science and Technology (19fksy0111); Anhui Province Key Laboratory of Environment-friendly Polymer Materials (KF2019001); the European Union's Horizon 2020 research and innovation programme under the Marie Skłodowska-Curie grant agreement No 744817; STCSM; China Postdoctoral Science Foundation (2015M571917, 2017T100442).

References

[1] Perumal P,Wang C S, Boopathi K M, Haider G W, Liao C and Chen Y F 2017 *Acs Photonics* **4**

[2] Yang S C, Wang Y and Sun H D 2015 *Adv. Optical Mater.* **3** 1136-1162

[3] Anand V R, Mathew S, Samuel B, Radhakrishnan P and Kailasnath M 2017 *Opt. Lett.* **42** 2926-2929

[4] Chen R, Ta V D and Sun H D 2014 *Acs Photonics* **1** 11-16

[5] Sandoghdar V V, Treussart F, Hare J, Lefèvre-Seguin V V, Raimond J and Haroche S 1996 *Phys. Rev. A* **54** R1777

[6] Linslal C L, Kailasnath M, Mathew S, Nideep T K, Radhakrishnan P, Nampoori V P and Vallabhan C P G 2016 *Opt. Lett.* **41** 551-554

[7] Vahala K J 2003 *Nature* **424** 839-846
[8] Zhu J D, Zhong Y and Liu H D 2017 *Photonics Res.* **5** 396
[9] Garrett C G, Kaiser W and Bond W L 1961 *Phys. Rev.* **124** 1807-1809
[10] Moon H J, Sun S P, Park G W, Lee J H and An K 2003 *J. Appl. Phys.* **42** L652-L654
[11] Ursaki V V, Burlacu A, Rusu E V, Postolake V and Tiginyanu I M 2009 *J. Opt. A-PURE Appl. Op.* **11** 075001
[12] Minamisawa R A, Süess M J, Spolenak R, Faist J, David C, Gobrecht J, Bourdelle K K and Sigg *H* 2012 *Nature Communications* **3** 1096
[13] Ta V D, Rui C and Han D S *Sci. Rep.* 2013 **3** 1362
[14] Kushida S, Okada D, Sasaki F, Lin Z H, Huang J S and Yamamoto Y 2017 *Adv. Optical Mater.* **5** 1700123
[15] Xu Z Z, Liao Q, Wang X D and Fu H B 2015 *Adv. Optical Mater.* **2** 1160-1166
[16] Jewell J L and Scherer 1990 *A Opt. Eng.* **29** 210-214
[17] Chen X, Zhang C, Webb D J, Kalli K and Peng G D 2010 *IEEE Photon. Technol. Lett.* **22** 850-852
[18] Yang L and Vahala K J 2003 *Opt. Lett.* **28** 592
[19] Yang Y, Lei F C, Kasumie S, Xu L H, Ward M, Yang L and chormaic S N 2017 *Opt. Express* **25** 1308
[20] Krämmer S, Vannahme C, Smith C L C, Grossmann T, Jenne M, Schierle S, Jørgensen L, Chronakis I S, Kristensen A and Kalt H 2014 *Adv. Mater.* **26** 8096-86100
[21] Huang D F, Li T S, Liu S Y, Yi T, Wang C K, Li J, Liu X Y and Xu M 2017 *Laser Phys.* **27** 035802
[22] Fang D, Chang C, Hsiao B S and And B C 2006 *Acs Symposium* **918** 91-105
[23] Xia D Y, Li D, Luo Y and Brueck S 2010 *Adv. Mater.* **18** 930-933
[24] Krämmer S, Laye F, Friedrich F, Vannahme C, Smith C L C, Mendes A C, Chronakis I S, Lahann J, Kristensen A and Kalt H 2017 *Adv. Optical Mater.* **5** 1700248
[25] Li D, Mccann J T, Xia Y and Marquez M 2010 *J. Am. Ceram. Soc.* **89** 1861-1869
[26] Zhang Y X, Pu X Y, Feng L, Han D Y and Ren Y T 2013 *Opt. Express* **21** 12617-28
[27] Djafar K M and Lowell L S 2002 *Science Press*
[28] Hall D G 1996 *Opt. Lett.* **21** 9-11
[29] Tang S K, Derda R, Quan Q, Lončar M and Whitesides G M 2011 *Opt. Express* **19** 2204-2215
[30] Lam C C, Leung P T and Young K 1992 *J. Opt. Soc. Am. B* **9** 1585-1592
[31] Ta V D, Chen R, Ma L, Ying Y J and Sun H D 2013 *Laser Photonics Rev.* **7** 133-139
[32] Peter J, Radhakrishnan P, Nampoori V P N and Kailasnath M 2014 *J. Lumin.* **149** 204-207
[33] He G S, Xu G C and Prasad P N 1995 *Opt. Lett.* **20** 435
[34]Chen R, Ta V D, Sun H D 2012 *Scientific Reports*, **2** 1-6
[35] Lin H B, Huston A L, Justus B L and Campillo A J 1986 *Opt. Lett.* **11** 614-616